
Multi-branch Attentive Transformer*

¹Yang Fan, ²Shufang Xie, ²Yingce Xia, ²Lijun Wu, ²Tao Qin, ¹Xiang-Yang Li, ²Tie-Yan Liu

¹ University of Science and Technology of China ² Microsoft Research Asia

¹fyabc@mail.ustc.edu.cn, xiangyangli@ustc.edu.cn

²{shufxi,yingce.xia,lijun.wu,taoqin,tyliu}@microsoft.com

Abstract

While the multi-branch architecture is one of the key ingredients to the success of computer vision tasks, it has not been well investigated in natural language processing, especially sequence learning tasks. In this work, we propose a simple yet effective variant of Transformer [26] called multi-branch attentive Transformer (briefly, MAT), where the attention layer is the average of multiple branches and each branch is an independent multi-head attention layer. We leverage two training techniques to regularize the training: drop-branch, which randomly drops individual branches during training, and proximal initialization, which uses a pre-trained Transformer model to initialize multiple branches. Experiments on machine translation, code generation and natural language understanding demonstrate that such a simple variant of Transformer brings significant improvements. Our code is available at <https://github.com/HA-Transformer>.

1 Introduction

The multi-branch architecture of neural networks, where each block consists of more than one parallel components, is one of the key ingredients to the success of deep neural models and has been well studied in computer vision. Typical structures include the inception architectures [24, 25, 23], ResNet [6], ResNeXt [32], DenseNet [8], and the network architectures discovered by neural architecture search algorithms [18, 13]. Models for sequence learning, a typical natural language processing problem, also benefit from multi-branch architectures. Bi-directional LSTM (BiLSTM) models can be regarded as a two-branch architecture, where a left-to-right LSTM and a right-to-left LSTM are incorporated into one model. BiLSTM has been applied in neural machine translation (briefly, NMT) [34, 31] and pre-training [17]. Transformer [26], the state-of-the-art model for sequence learning, also leverages multi-branch architecture in its multi-head attention layers.

Although multi-branch architecture plays an important role in Transformer, it has not been well studied and explored. Specifically, using hybrid structures with both averaging and concatenation operations, which has been widely used in image classification tasks [32, 25], are missing in current literature for sequence learning. This motivates us to explore along this direction. We propose a simple yet effective variant of Transformer, which treats a multi-head attention layer as a branch, duplicates such an attention branch for multiple times, and averages the outputs of those branches. Since both the concatenation operation (for the multiple attention heads) and the averaging operation (for the multiple attention branches) are used in our model, we call our model *multi-branch attentive Transformer* (briefly, MAT) and such an attention layer with both the concatenation and adding operations as the multi-branch attention layer.

Due to the increased structure complexity, it is challenging to directly train MAT. Thus, we leverage two techniques for MAT training. (1) *Drop branch*: During training, each branch should be independently dropped so as to avoid possible co-adaption between those branches. Note that similar to

*This work is conducted at Microsoft Research Asia.

Dropout, during inference, all branches are used. (2) *Proximal initialization*: We initialize MAT with the corresponding parameters trained on a standard single-branch Transformer.

Our contributions are summarized as follows:

- (1) We propose a simple yet effective variant of Transformer, multi-branch attentive Transformer (MAT). We leverage two techniques, drop branch and proximal initialization, to train this new variant.
- (2) We conduct experiments on three sequence learning tasks: neural machine translation, code generation and natural language understanding. On these tasks, MAT significantly outperforms the standard Transformer baselines, demonstrating the effectiveness of our method.
- (3) We explore another variant which introduces multiple branches into feed-forward layers. We find that such a modification slightly hurts the performance.

2 Background

2.1 Introduction to Transformer

A Transformer model consists of an encoder and a decoder. Both the encoder and the decoder are stacks of blocks. Each block is mainly made up of two types of layers: the multi-head attention layer and the feed-forward layer (briefly, FFN). We will mathematically describe them.

Let $\text{concat}(\dots)$ denote the concatenation operation, where all inputs are combined into a larger matrix along the last dimension. Let attn_M and attn denote a multi-head attention layer with M heads ($M \in \mathbb{Z}_+$) and a standard attention layer. A standard attention layer [3, 26] takes three elements as inputs, including query Q , key K and value V , whose sizes are $T_q \times d$, $T \times d$ and $T \times d$ (T_q, T, d are integers). attn is defined as follows:

$$\text{attn}(Q, K, V) = \text{softmax}\left(\frac{QK^\top}{\sqrt{d}}\right)V, \quad (1)$$

where softmax is the softmax operation. A multi-head attention layer aggregates multiple attention layers in the concatenation way:

$$\text{attn}_M(Q, K, V) = \text{concat}(H_1, H_2, \dots, H_M); H_i = \text{attn}(QW_Q^i, KW_K^i, VW_V^i), i \in [M], \quad (2)$$

where $[M]$ denotes the set $\{1, 2, \dots, M\}$. In Eqn.(2), the W 's are the parameters to be learned. Each W is of dimension $T \times (d/M)$. The output of attn_M is the same size as Q , i.e., $T_q \times d$.

In standard Transformer, an FFN layer, denoted by FFN , is implemented as follows:

$$\text{FFN}(x) = \max(xW_1 + b_1, 0)W_2 + b_2, \quad (3)$$

where x is a $1 \times d$ -dimension input, \max is an element-wise operator, W_1 and W_2 are $d \times d_h$ and $d_h \times d$ matrices, b_1 and b_2 are d_h and d dimension vectors. Usually, $d_h > d$.

In the encoder of a Transformer, each block consists of a self-attention layer, implemented as a attn_M where the query Q , key K and value V are the outputs of previous layer, and an FFN layer. In the decoder side, an additional multi-head attention is inserted between the self-attention layer and FFN layer, which is known as the encoder-decoder attention: Q is the output of the previous block, K and V are the outputs of the last block in the encoder.

2.2 Multi-branch architectures for sequence learning

As shown in Section 1, multi-branch architectures have been well investigated in image processing. In comparison, the corresponding work for sequence learning is limited. The bidirectional LSTM, a two-branch architecture, has been applied in machine translation [34, 31] and pre-training techniques like ELMo [17]. [21] proposed to use both convolutional neural networks and Transformer in the encoder and decoder. Similar idea is further expanded in [33]. A common practice of the previous work is that they focus on which network components (convolution, attention, etc.) should be used in a multi-branch architecture. In this work, we do not want to introduce additional operations into Transformer but focus on how to boost Transformer with its own components, especially, where and how to apply the multi-branch topology, and figure out several useful techniques to train multi-branch architectures for sequence learning. Such aspects are missing in previous literature.

3 Multi-branch attentive Transformer

In this section, we first introduce the structure of multi-branch attentive Transformer (MAT) in Section 3.1, and then we introduce the drop branch technique in Section 3.2. The proximal initialization is described in Section 3.3.

3.1 Network architecture

The network architecture of our proposed MAT adopts the backbone of standard Transformer, except that all multi-head attention layers (including both self-attention layers and encoder-decoder attention layers) are replaced with the *multi-branch attention layers*.

Let $\text{mAttn}_{N_a, M}(Q, K, V)$ denote a multi-branch attention layer, where N_a represents the number of branches and each branch is a multi-head attention layer with M heads attn_M . Q, K and V denote query, key and value, which are defined in Section 2. Mathematically, $\text{mAttn}_{N_a, M}(Q, K, V)$ works as follows:

$$\text{mAttn}_{N_a, M}(Q, K, V) = Q + \frac{1}{N_a} \sum_{i=1}^{N_a} \text{attn}_M(Q, K, V; \theta_i), \quad (4)$$

where $\theta_i = \{W_Q^i, W_K^i, W_V^i\}_{i=1}^M$ (see Eqn.(2)) is the collection of all parameters of the i -th multi-head attention layer.

3.2 Drop branch technique

As mentioned above, multiple branches in multi-branch attention layers have the same structure. To avoid the co-adaptation among them, we leverage the drop branch technique. The inspiration comes from the dropout [22] and drop path technique [12], where some branches are randomly dropped during training.

Let $\text{mAttn}_{N_a, M}(Q, K, V; \rho)$ denote a multi-branch attention layer with drop branch rate $\rho \in [0, 1]$, which is an extension of that in Section 3.1. Equipped with drop branch technique, the i -th branch of the multi-branch attention layer, denoted as $\beta_i^M(Q, K, V; \rho, \theta_i)$, works as follows:

$$\beta_i^M(Q, K, V; \rho, \theta_i) = \frac{\mathbb{I}\{U_i \geq \rho\}}{1 - \rho} \text{attn}_M(Q, K, V; \theta_i), \quad (5)$$

where U_i is uniformly sampled from $[0, 1]$ (briefly, $U_i \sim \text{unif}[0, 1]$); \mathbb{I} is the indicator function. During training, we may set $\rho \geq 0$, where any branch might be skipped with probability ρ . During inference, we must set $\rho = 0$, where all branches are leveraged with equal weights 1. The multi-branch attention layer $\text{mAttn}_{N_a, M}(Q, K, V; \rho)$ works as follows:

$$\text{mAttn}_{N_a, M}(Q, K, V; \rho) = Q + \frac{1}{N_a} \sum_{i=1}^{N_a} \beta_i^M(Q, K, V; \rho, \theta_i). \quad (6)$$

Note when $\rho = 0$, Eqn.(6) degenerates to Eqn.(4).

During training, it is possible that all branches in multi-branch attention layer are dropped. The residual connection ensures that even if all branches are dropped, the output from the previous layer can be fed to top layers through the identical mapping. That is, the network is never blocked. When $N_a = 1$ and $\rho = 0$, a multi-branch attention layer degenerates to a vanilla multi-head attention layer. When $N_a = 1$ and $\rho > 0$, it is the standard Transformer with randomly dropped attention layers during training, which is similar to the drop layer [5]. (See Section 4.2 for more discussions.)

We also apply the drop branch technique to FFN layers. That is, the revised FFN layer is defined as

$$x + \frac{\mathbb{I}\{U \geq \rho\}}{1 - \rho} \text{FFN}(x), \quad U \sim \text{unif}[0, 1] \quad (7)$$

where x is the output of the previous layer. An illustration of multi-branch attentive Transformer is in Figure 1. Each block in the encoder consists of a multi-branch attentive self-attention layer and an FFN layer. Each block in the decoder consists of another multi-branch attentive encoder-decoder attention layer. Layer normalization [2] remains unchanged.

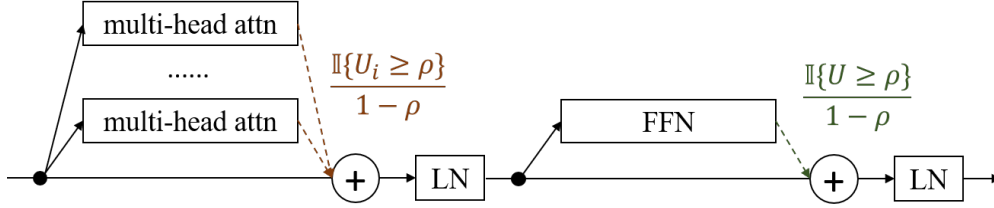


Figure 1: Architecture of a block in the encoder of MAT. “LN” refers to layer normalization.

3.3 Proximal initialization

MAT can be optimized like the standard version by first randomly initializing all parameters and training until convergence. However, the multi-branch attention layer increases the training complexity of MAT, since there are multiple branches to be optimized.

Recently, proximal algorithms [16] have been widely used in pretraining-and-finetuning framework to regularize training [9]. Then main idea of proximal algorithms is to balance the trade-off between minimizing the objective function and minimizing the weight distance with a pre-defined weight. Inspired by those algorithms, we design a two-stage warm-start training strategy:

- (1) Train a standard Transformer with embedding dimension d , FFN dimension d_h .
- (2) Duplicate both the self-attention layers and encoder-decoder attention layers for N_a times to initialize MAT. Train this new model until convergence.

We empirically find that the proximal initialization scheme can boost the performance than that obtained by training from scratch.

4 Application to neural machine translation

In this section, we conduct two groups of experiments: one with relatively small scale data, including IWSLT’14 German→English, IWSLT’14 Spanish↔English and IWSLT’17 French↔English translation tasks; the other with larger training corpus, WMT’14 English→German translation and WMT’19 German→French translation. We briefly denote English, German, Spanish and French as En, De, Es and Fr respectively.

4.1 Settings

Data preprocessing: Our implementation of NMT experiments is based on fairseq². For IWSLT’14 De↔En, we follow [4] to get and preprocess the training, validation and test data³, including lowercasing all words, tokenization and applying BPE [19]. For the other two IWSLT tasks, we do not lowercase the words and keep them case-sensitive. We apply tokenization and BPE as those used in preprocessing IWSLT De↔En. Training data sizes for IWSLT De→En, Es↔En and Fr↔En are 160k, 183k and 236k respectively. We choose IWSLT’13 Es↔En, IWSLT’16 Fr↔En for validation purpose, and choose IWSLT’14 Es↔En and IWSLT’17 Fr↔En as test sets. The numbers of BPE merge operation for the three tasks are all 10k. The source and target data are merged to get the BPE table.

For WMT’14 English→German translation, we follow [15] to preprocess the data, and eventually obtain 4.5M training data. We use newstest 2013 as the validation set, and choose newstest 2014 as the test set. The number of BPE merge operation is 32k. The preprocess steps for WMT’19 De→Fr are the same as those for WMT’14 En→De, and we eventually get 9M training data in total. We concatenate newstest2008 to newstest 2014 together as the validation set and use newstest 2019 as the test set.

Model configuration and training strategy: For the three IWSLT tasks, we choose the default setting provided by fairseq official code⁴ as the baseline with embedding dimension $d = 512$, hidden

²<https://github.com/pytorch/fairseq>

³The URLs of scripts we used in this paper are summarized in Appendix C.

⁴<https://github.com/pytorch/fairseq/blob/master/fairseq/models/transformer.py>

dimension $d_h = 1024$ and number of heads $M = 4$. For WMT’14 En→De, we mainly follow the big transformer setting, where the above three numbers are 1024, 4096 and 16 respectively. The dropout rates are 0.3. For the more detailed parameters like ρ and N_a , we will introduce the details in corresponding subsections. We use the Adam [10] optimizer with initial learning rate 5×10^{-4} , $\beta_1 = 0.9$, $\beta_2 = 0.98$ and the `inverse_sqrt` learning rate scheduler [26] to control training. Each model is trained until convergence. The source embedding, target embedding and output embedding of each task are shared. The batch size is 4096 for both IWSLT and WMT tasks. For IWSLT tasks, we train on single P40 GPU; for WMT tasks, we train on eight P40 GPUs.

Evaluation We evaluate the translation quality by BLEU scores. For IWSLT’14 De→En and WMT’14 En→De, following the common practice, we use `multi-bleu.perl`. For other tasks, we choose `sacreBLEU`.

4.2 Exploring hyper-parameters of MAT

Due to resource limitation, we first explore hyper-parameters and proximal initialization on IWSLT’14 De→En dataset to get some empirical results, then transfer them to larger datasets.

We try different combination of N_a , d and d_h . We ensure the number of total parameters not exceeding $36.7M$, the size of the default model for IWSLT’14 De→En. All results are reported in Table 1, where the network architecture is described by a four-element tuple, with each position representing the number of branches N_a , embedding dimension d , hidden dimension d_h and model sizes.

Table 1: Results on IWSLT’14 De→En with different architectures. The left and right subtables are experiments of standard transformer and MAT respectively. From left to right in each subtable, the columns represent the network architecture, number of parameters, BLEU scores with ρ ranging from 0.0 to 0.3.

$N_a/d/d_h/Param$	0.0	0.1	0.2	0.3	$N_a/d/d_h/Param$	0.0	0.1	0.2	0.3
Standard Transformer + Drop Branch					MAT + Drop Branch				
1/512/1024/36.7M	34.95 [△]	3.94	22.43	0.78	2/256/1024/18.4M	34.42	35.19	35.52	35.11
1/256/1024/13.7M	35.04	35.39	34.53	29.34	2/256/2048/24.7M	34.51	35.46	35.59	35.33
1/256/2048/20.0M	34.66	35.45	32.75	1.37	3/256/1024/23.1M	34.01	34.92	35.39	35.44
1/256/3072/26.3M	34.41	35.37	34.64	25.05	3/256/2048/29.4M	33.98	35.03	35.40	35.70
					4/256/1024/27.9M	33.77	34.84	35.08	35.14
					4/256/2048/34.2M	33.79	34.81	35.08	35.46

The baselines correspond to the architectures with $N_a = 1$ and $\rho = 0$. The most widely adopted baseline (marked with [△]) is 34.95 and the model size is 36.7M. Reducing d to 256 results in slightly BLEU score 35.04. We have the following observations:

(1) Using multi-branch attention layers with more than one branches can boost the translation BLEU scores, with a proper ρ . When setting $d_h = 1024$ and increasing N_a from 2 to 3, the BLEU scores are 35.52 (with $\rho = 0.2$) and 35.44 (with $\rho = 0.3$), outperforming the standard baseline 34.95, as well as the BLEU score obtained from architecture 1/256/1024. However, it is not always good to enlarge N_a . The BLEU score of MAT with $N_a = 4$ is 35.14, which is a minor improvement over the baseline.

Multi-branch attention layers also benefits from larger hidden dimension d_f . When setting $d_f = 2048$, we obtain consistent improvement compared to $d_f = 1024$ with the same N_a . Among all architectures, we find that the model 3/256/2048 achieves the best BLEU score, which is 35.70 (we also evaluate the validation perplexity of all architectures, and the model 3/256/2048 still get the lowest perplexity 4.71). Compared with the corresponding Transformer 1/256/2048 with $\rho = 0$, we get 1.04 improvement. We also enlarge ρ to 0.4 and 0.5, but the BLEU scores drop. Results are shown in Appendix A.

(2) The drop branch is important technique for training multi-branch attention layers. Take the network architecture 3/256/1024 as an example: If we do not use drop branch technique, i.e., $\rho = 0$, we can only get 34.01 BLEU score, which is 0.94 point below the baseline. As we increase ρ from 0 to 0.3, the BLEU scores become better and better, demonstrating the effectiveness of drop branch.

(3) When setting $N_a = 1$ and $\rho_B > 0$, the architecture still benefits from the drop branch technique. For architecture 1/256/1024, the vanilla baseline is 35.04. As we increase ρ to 0.1, we can obtain 0.35 point improvement. Wider networks with d_f also benefits from this technique, which shows that drop branch is generally a useful trick for Transformer. This is consistent with the discoveries in [5]. With $\rho = 0.1$, enlarging the hidden dimension to 2048 and 3072 lead to 35.45 and 35.37 BLEU scores, corresponding to 0.79 and 0.96 score improvements compared with that without using drop branch. But we found that when $N_a = 1$, drop branch might lead to unstable results. For example, when $\rho = 0.1$, 1/512/1024 cannot lead to a reasonable result. We re-run the experiments with five random seeds but always fail. In comparison, MAT can always obtain reasonable results with drop branch.

We also try to turn off the drop branch at the FFN layers. In this case, we found that by ranging ρ from 0 to 0.3, architecture 3/256/2048 can achieve 34.63, 34.78 and 34.98 BLEU scores, which are worse than those obtained by using drop branch at all layers. This shows that the drop branch at every layers is important for our proposed model.

4.3 Exploring proximal initialization

In this section, we explore the effect of proximal initialization, i.e., warm start from an existing standard Transformer model. The results are reported in Table 2. Generally, compared with the results without proximal initialization, the models can achieve more than 0.5 BLEU score improvement. Specifically, with $N_a = 3$ and $d_h = 2048$, we can achieve a 36.22 BLEU score, setting a state-of-the-art record on this task. We also evaluate the validation perplexity of all architectures in Table 2, and the model with $N_a = 3$ and $d_h = 2048$ still get the lowest perplexity 4.56.

Table 2: Results of using proximal initialization. Columns from left to right represent the network architecture, BLEU scores with drop branch ratio ρ from 0.0 to 0.3, and the increment compared to the best results without proximal initialization.

(N_a, d_h)	0.0	0.1	0.2	0.3	Δ
(2, 2048)	34.99	35.50	35.85	36.12	0.79
(3, 1024)	35.33	35.77	35.94	35.83	0.50
(3, 2048)	34.83	35.63	36.08	36.22	0.52
(4, 1024)	35.45	35.72	36.07	36.02	0.88
(4, 2048)	35.06	35.61	35.81	36.09	0.63

In summary, according to the exploration in Section 4.2 and Section 4.3, we empirically get the following conclusions: (1) A multi-branch attention layer is helpful to improve Transformer. We suggest to try $N_a = 2$ or $N_a = 3$ first. (2) A larger d_h is helpful to bring better performance. Enlarging d_h to consume the remaining parameters of reducing d (of the standard Transformer) is a better choice. (3) The drop branch and proximal initialization are two key techniques to the success of MAT in NMT.

4.4 Application to other NMT tasks

Results of other IWSLT tasks: We apply the discoveries to Spanish \leftrightarrow English and French \leftrightarrow English, and report the results in Table 3. For each setting, both the highest BLEU scores according to validation performance as well as the corresponding ρ 's are reported. We choose 1/512/1024 as the default baseline, whose model size is the upper bound of our MAT models. We also implement two other baselines, one with smaller d and the other with larger d_h . In baselines, the ρ is fixed as zero.

Compared to the standard Transformer with one branch, various MAT with different model configurations outperform the baseline. The architecture 2/256/2048 with $\rho = 0.2$ generally obtains promising results. Compared with the default baseline 1/512/1024, it achieves 1.74, 1.90, 1.31, 1.25 improvement on Es \rightarrow En, En \rightarrow Es, Fr \rightarrow En and En \rightarrow Fr.

Results on larger datasets: After obtaining results on small-scale datasets, we apply our discoveries to three larger datasets: WMT'14 En \rightarrow De translation, WMT'19 De \rightarrow Fr translation and WMT'19 En \rightarrow De translation.

Table 3: Results on IWSLT {Es, Fr} \leftrightarrow En.

$N_a/d/d_h$	#Params(M)	Es \rightarrow En / ρ	En \rightarrow Es / ρ	#Params(M)	Es \rightarrow En / ρ	En \rightarrow Es / ρ
1/512/1024	36.8	40.37 / 0.0	38.56 / 0.0	36.8	36.10 / 0.0	35.99 / 0.0
1/256/1024	13.7	40.60 / 0.0	39.42 / 0.0	13.7	36.21 / 0.0	36.16 / 0.0
1/256/2048	20.0	40.18 / 0.0	38.78 / 0.0	20.0	36.38 / 0.0	36.73 / 0.0
2/256/1024	18.4	41.02 / 0.1	39.56 / 0.1	18.4	36.37 / 0.2	36.57 / 0.2
2/256/2048	24.7	42.11 / 0.2	40.46 / 0.2	24.7	37.41 / 0.2	37.24 / 0.2
3/256/1024	23.1	41.39 / 0.1	40.08 / 0.2	23.2	37.44 / 0.2	37.30 / 0.1
3/256/2048	29.4	41.79 / 0.3	40.40 / 0.3	29.5	37.28 / 0.2	37.44 / 0.2

The results of WMT’14 En \rightarrow De are shown in Table 4. The standard baseline is 29.13 BLEU score, and the model contains 209.8M parameters. We implement an MAT with $N_a = 2$, $d_h = 12288$ and another with $N_a = 3$, $d_h = 10240$. We can see that our MAT also works for the large-scale dataset. When $N_a = 2$, we can obtain 29.90 BLEU score. When increasing N_a to 3, we can get 29.85, which is comparable with the the $N_a = 2$ variant. Besides, for large-scale datasets, the drop branch technique is important too. $\rho = 0.2$ works best of all settings.

Table 4: Results on WMT’14 En \rightarrow De translation.

$N_a/d/d_h$	#Param (M)	ρ	BLEU
1/1024/4096	209.8	0.0	29.08
1/512/10240	161.7	0.0	28.86
1/512/12288	186.9	0.0	28.95
2/512/12288	205.8	0.1	29.64
2/512/12288	205.8	0.2	29.90
2/512/12288	205.8	0.3	29.06
3/512/10240	199.5	0.1	29.62
3/512/10240	199.5	0.2	29.85
3/512/10240	199.5	0.3	29.05

We summarize previous results on WMT’14 En \rightarrow De in Table 5. MAT can achieve comparable or slightly better results than carefully designed architectures like weighted Transformer and DynamicConv, and than the evolved Transformer discovered by neural architecture search.

The results of WMT’19 De \rightarrow Fr are shown in Table 6. Compared with standard big transformer model of architecture 1/1024/4096, MAT with $\rho = 0.1$ can improve the baseline by 0.58 point.

Table 5: BLEU scores of WMT’14 En \rightarrow De in previous work.

Algorithm	BLEU
Weighted Transformer [1]	28.9
Evolved Transformer [20]	29.8
DynamicConv [30]	29.7
Our MAT	29.9

Table 6: Results on WMT’19 De \rightarrow Fr translation.

$N_a/d/d_h$	#Param (M)	ρ	BLEU
1/1024/4096	223.6	0.0	34.07
1/512/12288	193.7	0.0	33.90
2/512/12288	212.6	0.0	33.92
2/512/12288	212.6	0.1	34.65
2/512/12288	212.6	0.2	34.53
2/512/12288	212.6	0.3	34.49

Results with larger models: Finally, we explore whether our proposed MAT works for larger models. We conduct experiments on WMT’19 En \rightarrow De translation task. The data is downloaded from WMT’19 website⁵. We change the number of encoder layers to 12, set attention-dropout and activation-dropout as 0.1, and keep the other settings the same as WMT’14 En \rightarrow De. To validate the effectiveness of MAT, we evaluate the trained models on three test sets: WMT’14 En \rightarrow De, WMT’18 En \rightarrow De and WMT’19 En \rightarrow De. We use sacreBLEU to evaluate the translation quality. Furthermore, to facilitate comparison with previous work, we also use multi-bleu.perl to calculate the BLEU score for WMT’14 En \rightarrow De.

⁵The data is available at <http://www.statmt.org/wmt19/translation-task.html>. We concatenate Europarl v9, Common Crawl corpus, News Commentary v14 and Document-split Rapid corpus.

The results are shown in Table 7. Compared with the standard big transformer model of architecture 1/1024/4096, in terms of sacreBLEU, MAT with $\rho = 0.2$ can improve the baseline by 1.0, 1.0 and 1.1 points on WMT14, WMT18 and WMT19 test sets respectively. Specially, on WMT’14 En→De, in terms of multi-bleu, we achieve 30.8 BLEU score, setting a new record on this work under the supervised setting.

Table 7: Results of En→De with larger models. For WMT’14, both multi-bleu (left) and sacreBLEU (right) are reported.

$N_a/d/d_h$	#Param (M)	ρ	WMT14	WMT18	WMT19
1/1024/4096	325.7	0.0	29.8 / 29.2	42.7	39.3
1/512/12288	288.9	0.0	29.5 / 29.0	41.3	37.4
2/512/12288	314.1	0.0	30.0 / 29.6	42.5	38.5
2/512/12288	314.1	0.1	29.9 / 29.4	43.1	39.5
2/512/12288	314.1	0.2	30.8 / 30.2	43.7	40.4
2/512/12288	314.1	0.3	30.1 / 29.7	43.8	40.3

5 Application to code generation

We verify our proposed method on code generation, which is to map natural language sentences into code.

Datasets Following [29], we conduct experiments on a Java dataset⁶ [7] and a Python dataset [27]. In the Java dataset, the numbers of training, validation and test sequences are 69708, 8714 and 8714 respectively, and the corresponding numbers for Python are 55538, 18505 and 18502. All samples are tokenized. We use the downloaded Java dataset without further processing and use Python standard AST module to further process the python code. The source and target vocabulary sizes in natural language to Java code generation are 27k and 50k, and those for natural language to Python code generation are 18k and 50k. In this case, following [29], we do not apply subword tokenization like BPE to the sequences.

Model configuration We set $N_a = 4$, $d = 256$ and $d_h = 1024$ respectively. Both the encoder and the decoder consist of three blocks. The MAT model contains about 37M parameters. For the Transformer baseline, we set $d = 512$ and $d_h = 1024$, with 55M parameters.

Evaluation Following [29, 7], we use sentence-level BLEU scores, which is the average BLEU score of all sequences to evaluate the generation quality. We choose the percentage of valid code (PoV) as another metric for evaluation, which is the percentage of code that can be parsed into an AST.

We report the results on code generation task in Table 8. It is obvious that Transformer-based models (standard Transformer and MAT) is significantly better than the LSTM-based dual model. Compared with standard Transformer, our MAT can get 4.2 and 1.2 BLEU score improvement in Java and Python datasets respectively. MAT reaches the best BLEU scores when $\rho = 0.1$ on both on Java and Python datasets, which shows that the drop branch technique is important in code generation task. When $\rho = 0.1$, in terms of PoV, our MAT can boost the Transformer baseline by 5.8% and 6.6% points.

Table 8: Results on code generation.

Algorithm	Java		Python	
	BLEU	PoV	BLEU	PoV
Dual [29]	17.17	27.4%	12.09	51.9%
Transformer	23.30	83.1%	15.49	73.3%
Ours, $\rho = 0.0$	26.97	77.5%	16.35	65.5%
Ours, $\rho = 0.1$	27.53	88.9%	16.66	79.9%
Ours, $\rho = 0.2$	26.06	90.8%	15.63	84.0%
Ours, $\rho = 0.3$	24.72	90.2%	12.85	75.3%

⁶The urls of the datasets and tools we used for code generation are summarized in Appendix C.

6 Application to natural language understanding

We verify our proposed MAT on natural language understanding (NLU) tasks. Pre-training techniques have achieved state-of-the-art results on benchmark datasets/tasks like GLUE [28], RACE [11], etc. To use pre-training, a masked language model is first pre-trained on large amount of unlabeled data. Then the obtained model is used to initialize weights for downstream tasks. We choose RoBERTa [14] as the backbone. For GLUE tasks, we focus more on accuracy. Therefore, we do not control the parameters subconsciously. We set $N_a = 2$ for all experiments.

Following [5], we conduct experiments on MNLI-m, MRPC, QNLI and SST-2 tasks in GLUE benchmark [28]. SST-2 is a single-sentence task, which is to check whether the input movie review is a positive one or negative. The remaining tasks are two-sentence tasks. In MNLI, given a premise sentence and a hypothesis sentence, the task is to predict whether the premise entails the hypothesis (entailment), contradicts the hypothesis (contradiction), or neither (neutral). In MRPC, the task is to check whether the two inputs are matched. In QNLI, the task is to determine whether the context sentence contains the answer to the question. We choose the 24-layer RoBERTa_{large}⁷ to initialize our MAT. We report the validation accuracy following [5].

Table 9: Validation results on various NLU tasks. Results of RoBERTa and RoBERTa + LayerDrop (briefly, “+LayerDrop”) are from [5].

Algorithm	MNLI-m	MRPC	QNLI	SST-2
RoBERTa	90.2	90.9	94.7	96.4
+ LayerDrop	90.1	91.0	94.7	96.8
Ours	90.7	91.9	95.0	97.0

The results are reported in Table 9. Compared with vanilla RoBERTa model, on the four tasks MNLI-m, MRPC, QNLI and SST-2, we can improve them by 0.5, 1.0, 0.3 and 0.6 scores. Compared with the layer drop technique [5], we also achieve promising improvement on these four tasks. The results demonstrate that our method not only works for sequence generation tasks, but also for text classification tasks.

Drop branch also plays a central role on NLU tasks. We take the MRPC task as an example. The results are shown in Table 10. MRPC achieves the best result at $\rho = 0.3$.

Table 10: MRPC validation accuracy w.r.t. ρ .

ρ	0.1	0.2	0.3	0.4	0.5
accuracy	90.9	90.0	91.9	91.2	91.7

7 Exploring other variants

In this section, we first discuss whether applying multi-branch architectures to FFN layers is helpful. Then we discuss a new variant of drop branch technique. Finally we verify the importance of the multi-branch architecture, where both concatenation and averaging operations are used. We mainly conduct experiments on IWSLT tasks to verify the variants. We conduct experiments on IWSLT’14 De→En.

7.1 Multi-branch FFN layer

Algorithm: Denote the revised FFN layer as hFFN_{N_f} with $N_f (\in \mathbb{Z}_+)$ branches. Mathematically, given an input x from the previous layer,

$$\text{hFFN}_{N_f}(x) = x + \frac{1}{N_f} \sum_{i=1}^{N_f} \text{FFN}(x; \omega_i) \frac{\mathbb{I}\{U_i \geq \rho\}}{1 - \rho}, \quad (8)$$

⁷Models from page <https://github.com/pytorch/fairseq/tree/master/examples/roberta>.

where ω_i is the parameter of the i -th branch of the FFN layer, x is the output from the previous layer.

Experiments: We fix d as 256 and change N_f . We set the attention layers as both standard multi-head attention layers ($N_a = 1$) and multi-branch attention layers with $N_a = 2$. We set $N_f d_h = 2048$ to ensure the number of parameters unchanged with different number of branches. Results are reported in Table 11.

Table 11: Results on IWSLT’14 De→En with multi-branch FFN layers. From left to right, the columns represent the network architecture (with the number of parameters included), BLEU scores with ρ ranging from 0.0 to 0.3.

$N_a/N_f/d_h/\#Param$	0.0	0.1	0.2	0.3
1/1/2048/20.0M	34.66	35.45	32.75	1.37
1/2/1024/20.0M	34.85	35.38	35.30	34.39
1/4/512/20.0M	34.51	34.83	34.71	34.56
1/8/256/20.0M	34.35	34.36	34.38	33.86
2/1/2048/24.7M	34.51	35.46	35.59	35.33
2/2/1024/24.7M	34.39	35.18	35.55	35.42
2/4/512/24.7M	33.86	34.90	35.00	35.07
2/8/256/24.7M	34.05	34.59	34.70	34.55

We can see that increasing the branches of FFN layer while decreasing the corresponding hidden dimension (i.e., d_h) will hurt the performance. For standard Transformer with $N_a = 1$, as we increase N_f from 1 to 2, 4, 8, the BLEU scores drop from 35.45 to 35.38, 34.83 and 34.38. For MAT with $N_a = 2$, as N_f grows from 1 to 8, the BLEU decreases from 35.59 to 35.55, 35.00 and 34.70. That is, constraint by the number of total parameters, we do not need to separate FFN layers into multiple branches.

7.2 Variants of drop branch

Algorithm: In drop branch, the attention heads within a branch are either dropped together or kept together. However, we are not sure whether dropping a complete branch is the best choice. Therefore, we design a more general way to leverage dropout. Mathematically, the j -th attention head of the i -th branch, denoted as $\beta^{i,j}(Q, K, V; \rho, \theta_{i,j})$, works as follows:

$$\beta^{i,j}(Q, K, V; \rho, \theta_{i,j}) = \text{attn}(QW_Q^{i,j}, KW_K^{i,j}, VW_V^{i,j}) \frac{\mathbb{I}\{U_{i,j} \geq \rho\}}{1 - \rho}, \quad (9)$$

where superscripts i and j represent the branch id and head id in a multi-head attention layer respectively, $U^{i,j} \sim \text{unif}[0, 1]$, $\theta_{i,j} = \{W_Q^{i,j}, W_K^{i,j}, W_V^{i,j}\}$. Based on Eqn.(9), we can define a more general multi-branch attentive architecture:

$$\frac{1}{N_a} \sum_{i=1}^{N_a} \text{concat}(\beta^{i,1}(Q, K, V; \rho, \theta_{i,1}), \beta^{i,2}(Q, K, V; \rho, \theta_{i,2}), \dots, \beta^{i,M}(Q, K, V; \rho, \theta_{i,M})). \quad (10)$$

Keep in mind that Eqn.(10) is associated with $U^{i,j}$ for any $i \in [N_a], j \in [M]$. We apply several constraints to $U^{i,j}$, which can lead to different ways to regularize the training:

1. For any $i \in [N_a]$, sample $U^i \sim \text{unif}[0, 1]$ and set $U^{i,j} = U^i$ for any $j \in [M]$. This is the drop branch as we introduced in Section 3.1.
2. Each $U^{i,j}$ is independently sampled.

Experiments: We conduct experiments on IWSLT’14 De→En and the results are reported in Table 12. Proximal initialization is leveraged. From left to right, each column represents architecture, number of parameters, BLEU scores with ρ ranging from 0.0 to 0.3. The last column marked with Δ represents the improvement/decrease of the best results compared to those in Table 2.

We can see that randomly dropping heads leads to slightly worse results than the drop branch technique. Take the network architecture with $N_a = 3, d_h = 1024$ as an example. The best BLEU

Table 12: Results on IWSLT’14 De→En with randomly dropping heads technique. Embedding dimension d is fixed as 256.

(N_a, d_h)	0.0	0.1	0.2	0.3	Δ
(2, 2048)	34.99	35.53	35.95	35.96	-0.26
(3, 1024)	35.33	35.67	35.90	35.95	+0.01
(3, 2048)	34.83	35.45	35.76	36.07	-0.15
(4, 1024)	35.45	35.72	35.83	35.77	-0.24
(4, 2048)	35.06	35.79	35.72	36.03	-0.06

Table 13: Results on IWSLT’14 De→En with different numbers of heads.

ρ	0.1	0.2	0.3
$M = 1$	35.01	34.83	34.52
$M = 2$	35.11	35.45	35.15
$M = 4$	35.19	35.52	35.11

score that drop branch technique achieves is 36.22, and that obtained with randomly dropping heads is 36.07. Similarly observations can be found from other settings in Table 12. Therefore, we suggest to use the drop branch technique, which requires minimal revision to the benchmark code.

7.3 Ablation study on multi-branch attentions

MAT introduces multi-branch attention, in addition to the multi-head attention with the concatenation manner.⁸ It is interesting to know whether the multi-head attention is still needed given the multi-branch attention. We conduct experiments with $N_a = 2, d = 256, d_h = 1024$ and vary the number of heads M in `mAtttn $_{N_a, M}$` . Results are reported in Table 13.

We can see that the multi-head attention is still helpful. When $M = 1$, i.e., removing multiple heads and using a single head, it performs worse than multiple heads (e.g., $M = 4$). Therefore, the multi-branch of them is the best choice.

8 Conclusion and future work

In this work, we proposed a simple yet effective variant of Transformer called multi-branch attentive Transformer and leveraged two techniques, drop branch and proximal initialization, to train the model. Rich experiments on neural machine translation, code generation and natural language understanding tasks have demonstrated the effectiveness of our model.

For future work, we will apply our model to more sequence learning tasks. We will also combine our discoveries with neural architecture search, i.e., searching for better neural models for sequence learning in the search space with enriched multi-branch structures.

Appendix

A Exploring the Drop Branch in MAT

We explore more values of drop branch rate ρ , and the results are reported in Table 14.

From Table 14, we can see that increasing ρ to 0.4 and 0.5 will hurt the performance of MAT.

On IWSLT’14 De→En, with proximal initialization, we also explore increasing ρ to 0.4 and 0.5. The results are in Table 15. Still, setting ρ larger than 0.4 will hurt the performance.

B Exploration on Other IWSLT Tasks

B.1 Results of MAT

We apply the settings in Table 1 of the main paper to all four other IWSLT tasks. The results without proximal initialization are reported from Table 16 to Table 19. The results with proximal initialization are shown from Table 20 to Table 23.

⁸The multi-head attention in standard Transformer is also one kind of multi-branch attention. For simplicity, we use multi-head attention to denote the original attention layer in standard Transformer, and multi-branch attention to denote the newly introduced multi-branch attention in the multi-branch manner (both averaging and concatenation manner).

Table 14: Results on IWSLT’14 De→En with different architectures. From left to right, the columns represent the network architecture, number of parameters, BLEU scores with ρ ranging from 0.2 to 0.5. Results of $\rho = 0, 0.1$ are in Table 1 of the main text.

$N_a/d/d_h$ /Param	0.2	0.3	0.4	0.5
Standard Transformer + Drop Branch				
1/512/1024/36.7M	22.43	0.78	1.64	0.00
1/256/1024/13.7M	34.53	29.34	14.08	12.03
1/256/2048/20.0M	32.75	1.37	1.48	9.05
1/256/3072/26.3M	34.64	25.05	1.31	7.84
MAT + Drop Branch				
2/256/1024/18.4M	35.52	35.11	34.46	33.50
2/256/2048/24.7M	35.59	35.33	34.95	28.15
3/256/1024/23.1M	35.39	35.44	34.85	34.10
3/256/2048/29.4M	35.40	35.70	35.01	31.68
4/256/1024/27.9M	35.08	35.14	35.01	34.38
4/256/2048/34.2M	35.08	35.46	34.21	0.89

Table 15: Results of using proximal initialization. Columns from left to right represent the network architecture, BLEU scores with drop branch ratio ρ from 0.2 to 0.5, and the increment compared to the best results without proximal initialization.

(N_a, d_h)	0.2	0.3	0.4	0.5	Δ
(2, 2048)	35.85	36.12	35.62	35.03	0.79
(3, 1024)	35.94	35.83	35.76	35.15	0.50
(3, 2048)	36.08	36.22	35.87	35.58	0.52
(4, 1024)	36.07	36.02	35.78	35.42	0.88
(4, 2048)	35.81	36.09	35.80	35.57	0.63

Table 16: Results on IWSLT Es→En with different architectures. From left to right, the columns represent the network architecture, number of parameters, BLEU scores with ρ ranging from 0.0 to 0.3.

$N_a/d/d_h$ /Param	0.0	0.1	0.2	0.3
Standard Transformer + Drop Branch				
1/512/1024/36.7M	39.77 [△]	2.19	0.00	0.00
1/256/1024/13.7M	40.60	40.94	39.46	26.04
1/256/2048/20.0M	40.18	41.30	39.16	0.54
MAT + Drop Branch				
2/256/1024/18.4M	40.30	41.02	40.89	40.45
2/256/2048/24.7M	40.28	41.20	41.96	41.06
3/256/1024/23.1M	40.42	41.04	40.99	40.59
3/256/2048/29.4M	39.74	40.72	41.63	40.80
4/256/1024/27.9M	40.17	40.99	40.81	40.67
4/256/2048/34.2M	39.94	40.69	41.29	40.01

Table 17: Results on IWSLT En→Es with different architectures. From left to right, the columns represent the network architecture, number of parameters, BLEU scores with ρ ranging from 0.0 to 0.3.

$N_a/d/d_n$ /Param	0.0	0.1	0.2	0.3
Standard Transformer + Drop Branch				
1/512/1024/36.7M	38.56 [△]	1.67	0.01	0.00
1/256/1024/13.7M	39.51	39.58	38.42	23.50
1/256/2048/20.0M	38.78	39.84	38.22	0.90
MAT + Drop Branch				
2/256/1024/18.4M	38.81	39.56	38.98	39.08
2/256/2048/24.7M	38.77	39.33	39.86	39.37
3/256/1024/23.1M	38.31	39.12	39.77	39.29
3/256/2048/29.4M	38.22	39.89	39.57	39.90
4/256/1024/27.9M	38.37	39.16	39.55	39.49
4/256/2048/34.2M	38.40	39.05	39.24	39.35

Table 18: Results on IWSLT Fr→En with different architectures. From left to right, the columns represent the network architecture, number of parameters, BLEU scores with ρ ranging from 0.0 to 0.3.

$N_a/d/d_n$ /Param	0.0	0.1	0.2	0.3
Standard Transformer + Drop Branch				
1/512/1024/36.7M	36.60 [△]	2.09	0.01	0.01
1/256/1024/13.7M	36.21	36.17	35.15	3.99
1/256/2048/20.0M	36.38	36.42	35.11	14.66
MAT + Drop Branch				
2/256/1024/18.4M	35.63	36.28	36.37	35.61
2/256/2048/24.7M	35.90	35.83	36.34	36.08
3/256/1024/23.1M	35.72	35.71	36.11	35.59
3/256/2048/29.4M	35.55	36.30	36.22	36.27
4/256/1024/27.9M	35.52	36.30	36.06	36.12
4/256/2048/34.2M	34.98	36.67	36.24	35.97

Table 19: Results on IWSLT En→Fr with different architectures. From left to right, the columns represent the network architecture, number of parameters, BLEU scores with ρ ranging from 0.0 to 0.3.

$N_a/d/d_n$ /Param	0.0	0.1	0.2	0.3
Standard Transformer + Drop Branch				
1/512/1024/36.7M	36.32 [△]	36.07	0.02	0.05
1/256/1024/13.7M	36.16	36.43	35.61	0.79
1/256/2048/20.0M	36.73	36.80	35.34	1.59
MAT + Drop Branch				
2/256/1024/18.4M	36.41	36.48	36.57	36.34
2/256/2048/24.7M	35.95	37.20	36.90	36.44
3/256/1024/23.1M	35.79	36.52	36.56	36.34
3/256/2048/29.4M	35.88	36.88	36.88	36.86
4/256/1024/27.9M	35.77	36.68	37.09	36.50
4/256/2048/34.2M	35.23	36.65	36.97	36.66

Table 20: Results of using proximal initialization on IWSLT Es→En. Columns from left to right represent the network architecture, BLEU scores with drop branch ratio ρ from 0.0 to 0.3, and the increment compared to the best results without proximal initialization.

(N_a, d_h)	0.0	0.1	0.2	0.3	Δ
(2, 2048)	40.81	41.14	42.11	41.68	0.15
(3, 1024)	40.95	41.39	41.22	41.36	0.35
(3, 2048)	40.96	41.10	41.60	41.79	0.16
(4, 1024)	41.45	41.67	41.67	41.26	0.68
(4, 2048)	40.85	41.44	41.26	42.06	0.77

Table 21: Results of using proximal initialization on IWSLT En→Es. Columns from left to right represent the network architecture, BLEU scores with drop branch ratio ρ from 0.0 to 0.3, and the increment compared to the best results without proximal initialization.

(N_a, d_h)	0.0	0.1	0.2	0.3	Δ
(2, 2048)	39.47	39.78	40.46	40.34	0.60
(3, 1024)	39.47	40.06	40.08	39.84	0.31
(3, 2048)	39.34	39.61	40.08	40.40	0.50
(4, 1024)	39.36	39.99	39.81	40.00	0.45
(4, 2048)	39.75	40.16	40.12	39.91	0.81

Table 22: Results of using proximal initialization on IWSLT Fr→En. Columns from left to right represent the network architecture, BLEU scores with drop branch ratio ρ from 0.0 to 0.3, and the increment compared to the best results without proximal initialization.

(N_a, d_h)	0.0	0.1	0.2	0.3	Δ
(2, 2048)	36.14	36.76	37.41	36.82	0.77
(3, 1024)	36.73	37.03	37.44	37.10	1.33
(3, 2048)	36.32	36.92	37.28	37.25	0.98
(4, 1024)	36.81	37.14	37.10	36.88	0.73
(4, 2048)	36.48	36.90	37.40	37.29	0.73

Table 23: Results of using proximal initialization on IWSLT En→Fr. Columns from left to right represent the network architecture, BLEU scores with drop branch ratio ρ from 0.0 to 0.3, and the increment compared to the best results without proximal initialization.

(N_a, d_h)	0.0	0.1	0.2	0.3	Δ
(2, 2048)	36.73	37.14	37.24	37.09	0.04
(3, 1024)	36.71	37.30	37.04	36.92	0.74
(3, 2048)	36.51	37.39	37.44	37.43	0.56
(4, 1024)	36.67	36.77	37.24	37.15	0.15
(4, 2048)	36.70	37.19	37.18	37.32	0.35

B.2 Variants of Drop Branch

We explore the variant of drop branch described in Section 7.2 on the other four IWSLT tasks. We apply all settings in Table 11 of the main paper to the remaining language pairs. Results are reported from Table 24 to Table 27. Generally, the two types of drop branch achieve similar results.

Table 24: Results on IWSLT Es→En with randomly dropping heads technique. Embedding dimension d is fixed as 256.

(N_a, d_h)	0.0	0.1	0.2	0.3	Δ
(2, 2048)	40.81	41.61	41.54	41.68	-0.43
(3, 1024)	40.95	41.63	41.25	41.15	+0.24
(3, 2048)	40.96	41.30	41.39	41.86	+0.07
(4, 1024)	41.45	41.41	41.04	41.29	-0.22
(4, 2048)	40.85	41.30	41.48	41.70	-0.36

Table 25: Results on IWSLT En→Es with randomly dropping heads technique. Embedding dimension d is fixed as 256.

(N_a, d_h)	0.0	0.1	0.2	0.3	Δ
(2, 2048)	39.47	39.85	39.98	40.39	-0.07
(3, 1024)	39.47	39.99	39.96	39.41	-0.09
(3, 2048)	39.34	39.47	40.22	39.67	-0.18
(4, 1024)	39.36	39.71	39.59	39.89	-0.11
(4, 2048)	39.75	39.73	39.94	40.36	+0.20

Table 26: Results on IWSLT Fr→En with randomly dropping heads technique. Embedding dimension d is fixed as 256.

(N_a, d_h)	0.0	0.1	0.2	0.3	Δ
(2, 2048)	36.14	37.10	36.85	36.71	-0.31
(3, 1024)	36.73	36.78	36.83	36.20	-0.61
(3, 2048)	36.32	36.73	36.92	37.08	-0.20
(4, 1024)	36.81	36.29	36.82	36.49	-0.32
(4, 2048)	36.48	36.39	36.89	36.99	-0.41

Table 27: Results on IWSLT En→Fr with randomly dropping heads technique. Embedding dimension d is fixed as 256.

(N_a, d_h)	0.0	0.1	0.2	0.3	Δ
(2, 2048)	36.73	37.18	37.48	37.15	+0.24
(3, 1024)	36.71	37.14	37.48	36.86	+0.18
(3, 2048)	36.51	36.93	37.17	36.97	-0.27
(4, 1024)	36.67	36.59	37.02	36.99	-0.22
(4, 2048)	36.70	36.81	37.80	37.37	+0.48

C Scripts

In this section, we summarize the scripts we used in our paper.

(1) multi-bleu.perl: <https://github.com/moses-smt/mosesdecoder/blob/master/scripts/generic/multi-bleu.perl>

(2) sacreBLEU: <https://github.com/mjpost/sacreBLEU>

- (3) The script to preprocess the IWSLT data: <https://github.com/pytorch/fairseq/blob/master/examples/translation/prepare-iwslt14.sh>
- (4) Path to Java dataset: <https://github.com/xing-hu/TL-CodeSum>
- (5) Path to Python dataset: https://github.com/wanyao1992/code_summarization_public
- (6) Python standard AST module to process the Python code: <https://docs.python.org/3/library/ast.html>

References

- [1] Karim Ahmed, Nitish Shirish Keskar, and Richard Socher. Weighted transformer network for machine translation. *arXiv preprint arXiv:1711.02132*, 2017.
- [2] Jimmy Lei Ba, Jamie Ryan Kiros, and Geoffrey E Hinton. Layer normalization. *arXiv preprint arXiv:1607.06450*, 2016.
- [3] Dzmitry Bahdanau, Kyunghyun Cho, and Yoshua Bengio. Neural machine translation by jointly learning to align and translate. *ICLR*, 2015.
- [4] Sergey Edunov, Myle Ott, Michael Auli, David Grangier, and Marc’Aurelio Ranzato. Classical structured prediction losses for sequence to sequence learning. *NAACL*, 2018.
- [5] Angela Fan, Edouard Grave, and Armand Joulin. Reducing transformer depth on demand with structured dropout. In *International Conference on Learning Representations*, 2020.
- [6] Kaiming He, Xiangyu Zhang, Shaoqing Ren, and Jian Sun. Deep residual learning for image recognition. In *Proceedings of the IEEE conference on computer vision and pattern recognition*, pages 770–778, 2016.
- [7] Xing Hu, Ge Li, Xin Xia, David Lo, Shuai Lu, and Zhi Jin. Summarizing source code with transferred api knowledge. In *Proceedings of the Twenty-Seventh International Joint Conference on Artificial Intelligence, IJCAI-18*, pages 2269–2275. International Joint Conferences on Artificial Intelligence Organization, 7 2018.
- [8] Gao Huang, Zhuang Liu, Laurens Van Der Maaten, and Kilian Q Weinberger. Densely connected convolutional networks. In *Proceedings of the IEEE conference on computer vision and pattern recognition*, pages 4700–4708, 2017.
- [9] Haoming Jiang, Pengcheng He, Weizhu Chen, Xiaodong Liu, Jianfeng Gao, and Tuo Zhao. Smart: Robust and efficient fine-tuning for pre-trained natural language models through principled regularized optimization, 2019.
- [10] Diederik P Kingma and Jimmy Ba. Adam: A method for stochastic optimization. *ICLR*, 2015.
- [11] Guokun Lai, Qizhe Xie, Hanxiao Liu, Yiming Yang, and Eduard Hovy. Race: Large-scale reading comprehension dataset from examinations. *arXiv preprint arXiv:1704.04683*, 2017.
- [12] Gustav Larsson, Michael Maire, and Gregory Shakhnarovich. Fractalnet: Ultra-deep neural networks without residuals. *ICLR*, 2017.
- [13] Hanxiao Liu, Karen Simonyan, and Yiming Yang. Darts: Differentiable architecture search. In *7th International Conference on Learning Representations*, 2019.
- [14] Yinhan Liu, Myle Ott, Naman Goyal, Jingfei Du, Mandar Joshi, Danqi Chen, Omer Levy, Mike Lewis, Luke Zettlemoyer, and Veselin Stoyanov. Roberta: A robustly optimized bert pretraining approach. *ICLR*, 2019.
- [15] Myle Ott, Sergey Edunov, David Grangier, and Michael Auli. Scaling neural machine translation. *arXiv preprint arXiv:1806.00187*, 2018.
- [16] Neal Parikh and Stephen Boyd. *Proximal Algorithm*. Now Publishers, Inc., 2013.
- [17] Matthew E Peters, Mark Neumann, Mohit Iyyer, Matt Gardner, Christopher Clark, Kenton Lee, and Luke Zettlemoyer. Deep contextualized word representations. *NAACL*, 2018.
- [18] Hieu Pham, Melody Y Guan, Barret Zoph, Quoc V Le, and Jeff Dean. Efficient neural architecture search via parameter sharing. *arXiv preprint arXiv:1802.03268*, 2018.
- [19] Rico Sennrich, Barry Haddow, and Alexandra Birch. Neural machine translation of rare words with subword units. *ACL*, 2016.

- [20] David R So, Chen Liang, and Quoc V Le. The evolved transformer. *ICML*, 2019.
- [21] Kaitao Song, Xu Tan, Di He, Jianfeng Lu, Tao Qin, and Tie-Yan Liu. Double path networks for sequence to sequence learning. *COLING*, 2018.
- [22] Nitish Srivastava, Geoffrey Hinton, Alex Krizhevsky, Ilya Sutskever, and Ruslan Salakhutdinov. Dropout: a simple way to prevent neural networks from overfitting. *The journal of machine learning research*, 15(1):1929–1958, 2014.
- [23] Christian Szegedy, Sergey Ioffe, Vincent Vanhoucke, and Alexander A Alemi. Inception-v4, inception-resnet and the impact of residual connections on learning. In *Thirty-First AAAI Conference on Artificial Intelligence*, 2017.
- [24] Christian Szegedy, Wei Liu, Yangqing Jia, Pierre Sermanet, Scott Reed, Dragomir Anguelov, Dumitru Erhan, Vincent Vanhoucke, and Andrew Rabinovich. Going deeper with convolutions. In *Proceedings of the IEEE conference on computer vision and pattern recognition*, pages 1–9, 2015.
- [25] Christian Szegedy, Vincent Vanhoucke, Sergey Ioffe, Jon Shlens, and Zbigniew Wojna. Rethinking the inception architecture for computer vision. In *Proceedings of the IEEE conference on computer vision and pattern recognition*, pages 2818–2826, 2016.
- [26] Ashish Vaswani, Noam Shazeer, Niki Parmar, Jakob Uszkoreit, Llion Jones, Aidan N Gomez, Łukasz Kaiser, and Illia Polosukhin. Attention is all you need. In *Advances in neural information processing systems*, pages 5998–6008, 2017.
- [27] Yao Wan, Zhou Zhao, Min Yang, Guandong Xu, Haochao Ying, Jian Wu, and Philip S Yu. Improving automatic source code summarization via deep reinforcement learning. In *Proceedings of the 33rd ACM/IEEE International Conference on Automated Software Engineering*, pages 397–407, 2018.
- [28] Alex Wang, Amanpreet Singh, Julian Michael, Felix Hill, Omer Levy, and Samuel R. Bowman. GLUE: A multi-task benchmark and analysis platform for natural language understanding. In *International Conference on Learning Representations*, 2019.
- [29] Bolin Wei, Ge Li, Xin Xia, Zhiyi Fu, and Zhi Jin. Code generation as a dual task of code summarization. In *Advances in Neural Information Processing Systems*, pages 6559–6569, 2019.
- [30] Felix Wu, Angela Fan, Alexei Baevski, Yann Dauphin, and Michael Auli. Pay less attention with lightweight and dynamic convolutions. In *International Conference on Learning Representations*, 2019.
- [31] Yonghui Wu, Mike Schuster, Zhifeng Chen, Quoc V Le, Mohammad Norouzi, Wolfgang Macherey, Maxim Krikun, Yuan Cao, Qin Gao, Klaus Macherey, et al. Google’s neural machine translation system: Bridging the gap between human and machine translation. *arXiv preprint arXiv:1609.08144*, 2016.
- [32] Saining Xie, Ross Girshick, Piotr Dollár, Zhuowen Tu, and Kaiming He. Aggregated residual transformations for deep neural networks. In *Proceedings of the IEEE conference on computer vision and pattern recognition*, pages 1492–1500, 2017.
- [33] Guangxiang Zhao, Xu Sun, Jingjing Xu, Zhiyuan Zhang, and Liangchen Luo. Muse: Parallel multi-scale attention for sequence to sequence learning. *arXiv preprint arXiv:1911.09483*, 2019.
- [34] Jie Zhou, Ying Cao, Xuguang Wang, Peng Li, and Wei Xu. Deep recurrent models with fast-forward connections for neural machine translation. *Transactions of the Association for Computational Linguistics*, 4:371–383, 2016.